

Effects of inorganic mercury exposure in the alveolar bone of rats: an approach of qualitative and morphological aspects

Paula Beatriz de Oliveira Nunes¹, Maria Karolina Martins Ferreira¹, Deborah Ribeiro Frazão¹, Leonardo Oliveira Bittencourt¹, Victória dos Santos Chemelo¹, Márcia Cristina Freitas Silva¹, Armando Lopes Pereira-Neto², Alan Rodrigo Leal Albuquerque³, Simone Patricia Aranha Paz³, Rômulo Simões Angélica³, Sofia Pessanha⁴ and Rafael Rodrigues Lima¹

¹Laboratory of Functional and Structural Biology, Institute of Biological Sciences, Federal University of Pará, Belém, Pará, Brazil

²School of Dentistry, Federal University of Pará, Belém, Pará, Brazil

³Institute of Geosciences, Federal University of Pará, Belém, Pará, Brazil

⁴Laboratory of Instrumentation, Biomedical Engineering and Radiation Physics, NOVA School of Sciences and Technology, Caparica, Portugal

ABSTRACT

Background: In comparison to organic mercury (MeHg), the environmental inorganic mercury (IHg) can be found in some skin-lightening cosmetics were considered “harmless” for a long time. However, recent studies have shown that long-term exposure to low doses of IHg may affect biological systems. Therefore, this study investigated the effects of IHg long-term exposure to the alveolar bone of adult rats.

Methods: Adult *Wistar* rats were distributed in control and HgCl₂ exposed (0.375 mg/kg/day). After 45 days, the rats were euthanized and both blood and hemimandibles were collected. Total blood Hg levels were measured and both inorganic and organic components of the alveolar bone were determined through XRD and ATR-FTIR. The microstructure of the alveolar bone was assessed by using micro-CT and the morphometric analysis was performed by using stereomicroscopy.

Results: Alterations in the physicochemical components of the alveolar bone of exposed animals were observed. The bone changes represented a tissue reaction at the microstructural level, such as bone volume increase. However, no significant dimensional changes (bone height) were observed.

Conclusion: Exposure to IHg at this dose can promote microstructural changes and alteration in the organic and inorganic components in the alveolar bone.

Subjects Biochemistry, Toxicology

Keywords Inorganic mercury, Mercury chloride, Alveolar bone, Rats, Infrared mineral characterization, Micro-computed tomography

INTRODUCTION

Mercury (Hg) is considered the 10th most harmful element to human health (*WHO, 2017*). Inorganic (elemental, inorganic salts, *e.g.*) and organic (methylmercury, dimethylmercury, *e.g.*) are the two primary Hg chemical forms, which can be

Submitted 4 August 2021
Accepted 9 November 2021
Published 26 January 2022

Corresponding author
Rafael Rodrigues Lima,
rafalima@ufpa.br

Academic editor
Joao Rocha

Additional Information and
Declarations can be found on
page 11

DOI 10.7717/peerj.12573

© Copyright
2022 Nunes et al.

Distributed under
Creative Commons CC-BY 4.0

OPEN ACCESS

bioaccumulated in the biosphere through a dynamic biogeochemical cycle (Sakamoto, Nakamura & Murata, 2018; Siciliano et al., 2005).

Anthropogenic actions such as inappropriate industrial waste management and illegal artisanal gold mining resulted in Hg contamination of ecosystems and became a public health concern. It has been shown that Hg levels in commercially available fishes may reach up to 8.71 µg/g, of which 0.3 µg/g corresponds to inorganic Hg (IHg) (Rodríguez Martín-Doimeadios et al., 2014). Moreover, the significant increase in illegal Amazon deforestation corroborates the increase of Hg emission, which results in higher environmental contamination and human exposure to Hg (Crespo-Lopez et al., 2021).

It is worthwhile to consider that humans can be daily exposed to IHg through water, seafood, vegetables, and cosmetics (Park & Zheng, 2012; Risher & De Rosa, 2007; UNEP, 2013). In comparison to organic forms, the physical-chemical characteristics of IHg limit its absorption and body distribution. Hg compounds also present two different oxidation states named mercurous (Hg⁺) and mercuric (Hg⁺²), the latter of which has a high affinity for sulfhydryl groups that favors the absorption of IHg by albumin, glutathione, amino acids, and other proteins. Thus, IHg is transported by intestinal enterocytes and renal epithelial cells, reaches the systemic circulation, and is delivered to target organs (Bridges & Zalups, 2010, 2005, 2004; Ballatori, 2002).

Toxic effects of IHg have been observed in the hematopoietic system, salivary glands, and the central nervous system (Bernhoft, 2012; Rice et al., 2014; Aragão et al., 2018; Ahmad & Mahmood, 2019; Corrêa et al., 2020); however, there is scarce evidence on IHg toxicity on bone tissue such as the reduction of mineral density in long bones (Jin et al., 2002). Alveolar bone is a mineralized connective tissue derived from the ectomesenchyme. Besides supporting teeth (Zhou et al., 2018), this tissue plays a significant role in the distribution and absorption of occlusal forces that leads to the continuous bone remodeling process (Monje et al., 2015). It must be emphasized that this tissue has different responsiveness to bone resorption and remodeling and some mechanical and biochemical stimuli can alter both the quality and quantity of alveolar bone (Tanaka et al., 2002; Mavropoulos, Rizzoli & Ammann, 2007).

Only one study recently investigated the effects of MeHg exposure on the alveolar bone (de Oliveira Lopes et al., 2021); thus, this original study aimed to investigate the effects of IHg long-term exposure on the alveolar bone of adult rats.

MATERIALS AND METHODS

Animals and experimental groups

In this study, 20 Male Wistar rats (*Rattus norvegicus*), with 90 days old and 170–180 g, were obtained from an animal facility at the Federal University of Pará. The animals were simple randomized and allocated in collective cages with four animals per cage, where they received food and water *ad libitum*. Besides, the rats were submitted to 12 h of light/dark and maintained in a temperature-controlled room (25 ± 1 °C). All procedures were approved by the Ethics Committee on Experimental Animals of the Federal University of Pará (UFPA), under number 9228050418, according to NIH Guide for the

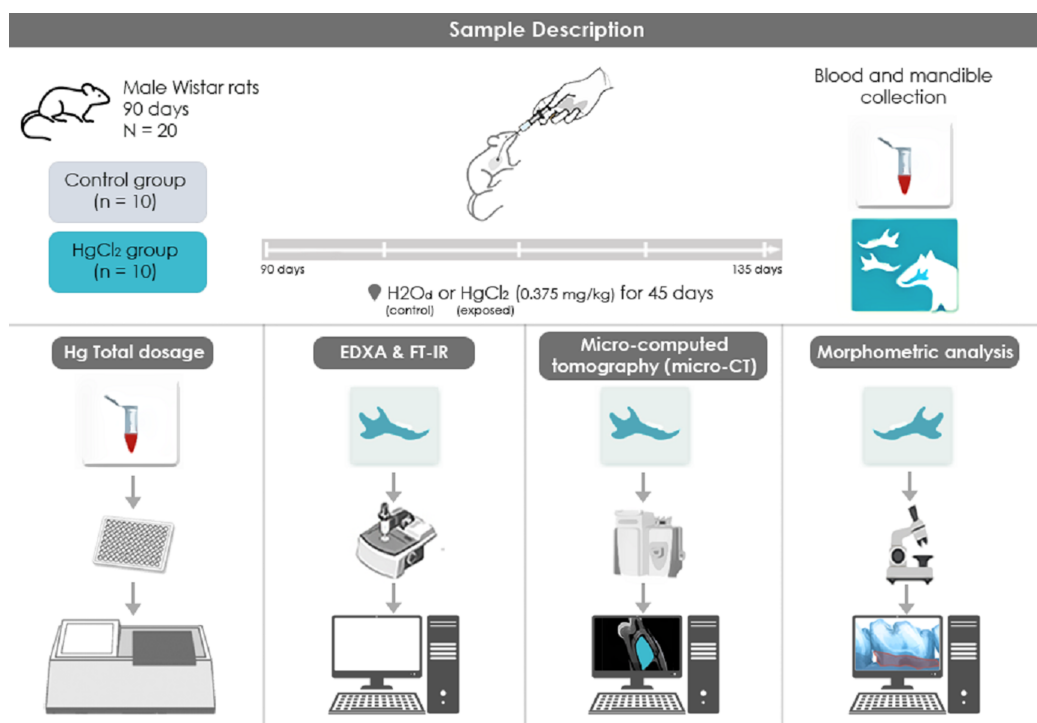


Figure 1 Sample description and experimental stages methodological figure of IHg exposure, experimental group division, and analyses performed. (1) HgCl₂ exposure to 0.375 mg/kg/day by intragastric gavage for 45 days; (2) euthanasia and biological sample collection procedures (blood and mandibles); (3) total mercury levels by atomic absorption spectrometry. (4) Physicochemical analysis of the alveolar bone through Fourier Transform Infrared Spectroscopy (FT-IR); (5) Micro-computed tomography (micro-CT) analyze and (6) alveolar bone morphometric analysis by stereomicroscope.

Full-size DOI: [10.7717/peerj.12573/fig-1](https://doi.org/10.7717/peerj.12573/fig-1)

Care and Use of Laboratory Animals recommendations and The ARRIVE guidelines (Percie du Sert *et al.*, 2020).

The mercury chloride (HgCl₂) was orally administered to the animals of this group ($n = 10$) with a concentration of 0.375 mg/kg for 45 days, adjusting the dose according to the animals' weight. We used the protocol that was previously established by our group (Teixeira *et al.*, 2014; Aragão *et al.*, 2017; Aragão *et al.*, 2018; Teixeira *et al.*, 2018; Teixeira *et al.*, 2019; Corrêa *et al.*, 2020). The control group ($n = 10$) received distilled water by intragastric gavage for the same period in proportional volumes. Twenty-four hours after the last HgCl₂ administration, the animals were euthanized with ketamine (90 mg/kg) and xylazine (10 mg/kg), and then the blood was collected for the Hg levels quantification. Also, mandibles were collected and divided for different analyses. Also, one hemimandible from each animal were maintained in saline solution (0.9%) stored in $-20\text{ }^{\circ}\text{C}$ refrigerator for mineral content analyses, while the other hemimandible was maintained in a 4% formalin solution for stereomicroscopic and microtomography analyses. For the FT-IR and XRD analyses, the alveolar bone was macerated until fine granulation powder was obtained, being then stored in different microtubes and destined for the respective analyses. All the methodological steps are summarized in Fig. 1.

Total Hg quantification

After blood collection through intracardiac puncture, the samples were centrifuged (3,000 rpm for 10 min) for plasma collection. Then, 1 mL of each sample was digested by an acid solution (nitric, perchloric and sulfuric, 1:1:5, v/v) and added to an electric hot plate at a temperature between 200–300 °C, and then the samples were analyzed in an atomic absorption spectrophotometer (Semi-Automatic Mercury Analyzer-Hg 201) to determine the total Hg levels, considering the detection limit 0.001 mg kg⁻¹. The results were expressed in µg/mL (*Dos Santos Chemelo et al., 2020*).

Crystallography analysis

The alveolar bone samples already prepared were destined for XRD analysis, which was performed using an X-Ray Diffractometer, model Empyrean from PANalytical, from the Laboratory of Mineral Characterization-X-Ray Sector. The equipment has an anode ceramic X-ray tube with Co (K α 1 = 1,789010 Å), long fine focus, Fe K β filter, PIXCEL3D-Medpix3 1 × 1 detector, in scanning mode. The analytics condition was with 40 kV voltage, 35 mA current, step size 0.0263° in 2 θ , scan from 3.00° to 95.00° in 2 θ , time/step 59.92 s, 1/8° of the divergent slit and 1/4° of anti-scattering, with 10 mm mask. Sample preparation was carried by micropreparation method using a silicon zero background sample holder.

The software X'Pert Data Collector 5.1 collected the data, and the software X'Pert HighScore Plus 4.7 made the data processing. The identification of minerals or crystalline phases was made by comparing the diffractogram obtained with standards (cards) from the ICDD-PDF (International Center for Diffraction Data–Powder Diffraction File) database.

Infrared mineral characterization (FT-IR)

After pretreatment, samples were dried at 60 °C for 24 h and destined for FT-IR analysis were in a performed Thermo Spectrometer (Nicolet iS50) in the 4,000–400 cm⁻¹ spectral range. Each spectrum is the sum of 100 scans with 4 cm⁻¹ resolution. The OMNIC software was used to obtain the data. As a pre-treatment, the samples were dried at 60 °C for 24 h and analyzed in the Attenuated Total Reflection (ATR) technique which performs direct non-destructive analysis of the solids. The vibrational values established were registered as proposed by *Lopes et al. (2018)*.

Micro-computed tomography analysis (micro-CT)

For this analysis, the hemimandibles were digitized and the alveolar bone was evaluated in it, by a cone-beam micro-CT system (Skyscan 1172; Bruker, Kontich, Belgium). The X-ray generator was operated at an accelerated 60 kV potential, with a 165 µA beam current and a 650 ms exposure time per projection. Images were produced with a voxel (6 × 6 × 6 mm). The region of interest (ROI) was outlined from the apexes of the second molar roots up to the roof of the first molar's furcation, touching the roots surfaces, in all images of the coronal dataset, using appropriate software (Data Viewer software,

Bruker-Skyscan). Percentage of bone volume (BV/TV); trabecular spacing (Tb.Sp; mm); trabecular number (Tb.N; mm^{-1}) and bone surface/volume ratio (Bs/TV) were the parameters analyzed.

Morphometric analysis

The left hemimandible was used to measure the area between the cemento-enamel junction (CEJ) and alveolar bone crest (ABC) of second molars. This measurement is considered a sensitive parameter of alveolar bone loss (Lopes Castro *et al.*, 2020; Frazão *et al.*, 2020). So, the hemimandibles were immersed in 8% sodium hypochlorite for 4 h, then washed in running water so that they could be immediately dried and immersed in 1% methylene blue (Sigma-Aldrich, St. Louis, MO, USA). Subsequently, we obtained the second molars' lingual surface exposed area images with a stereomicroscope (M205A; Leica, Wetzlar, Germany) and imaging software (LAS-X, Leica). The images' limits were the CEJ, ABC, mesial and distal surfaces of the second molars.

Statistical analyses

All data were inserted at GraphPad Prism 5.0 and submitted to the normality test. The method of Kolmogorov-Smirnov ($p > 0.10$) tested the data distribution. For the variables with normal distribution, the Student's *t*-test was used, considering a significant $p < 0.05$. For the body mass evaluation, the Two-way ANOVA test was applied by the Tukey test to perform a comparison between groups. The results were expressed graphically and numerically with mean and standard error (mean \pm standard error) for those showing parametric.

The power of the test was analyzed, calculating the difference between two mean by OpenEpi software (versão 2.3.1) adopting type I error of 5% and power of 80% (Table S1). The number of animals required for this experiment was calculated using the OpenEpi software, with criteria for analysis of variances, based on the study in 2021 by *de Oliveira Lopes et al.* (2021); the α err prob was 0.05, and a power of 0.80.

RESULTS

Exposure to IHg did not affect the animals' body weight

The animals were weighed weekly, and the animals in both groups gained weight ($p < 0.0001$). At the end of the experimental protocol, the animals in the control group and the exposed group (IHg) showed no difference in body weight (Control: 215.4 ± 8.457 ; IHg: 210.4 ± 7.372 , $p > 0.05$) (Fig. 2).

The long-term exposure to IHg increases total Hg bioavailability in adult rats

As a validation of our experimental design of Hg exposure, total Hg levels in blood were higher in exposure rats (0.048 ± 0.002 $\mu\text{g/mL}$) when compared to controls (values lower than the detection limits; $p < 0.0001$) (Fig. 3).

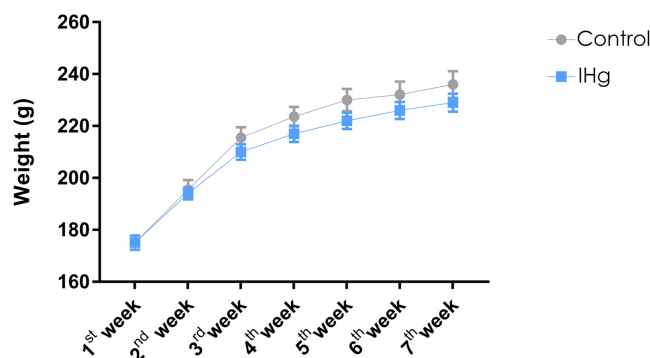


Figure 2 Effects of chronic exposure to IHg on body weight (g) of adult Wistar rats. Results are expressed as mean \pm standard error mean. No significant differences ($p > 0.05$) between groups at any time. Two-way ANOVA and Tukey's post-hoc test, $p < 0.05$.

Full-size DOI: 10.7717/peerj.12573/fig-2

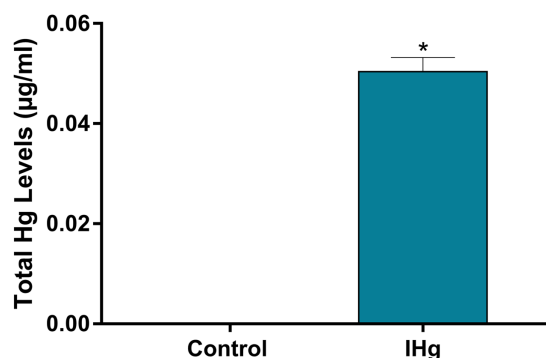


Figure 3 Total Hg (Hg) levels found in the plasma of adult Wistar rats after 45 days of exposure to 0.375 mg/kg/day of HgCl_2 . Results are expressed as mean \pm standard error mean (SEM). * $p < 0.05$ compared to the control group.

Full-size DOI: 10.7717/peerj.12573/fig-3

Changes in the parameters between groups were observed during the characterization of organic and inorganic components (FT-IR)

The FT-IR results showed different bands between the groups exposed to IHg (blue line) and the control group (red line). The FT-IR spectrum of the rats' alveolar bone exposed to IHg suggests modulation in the three vibrational modes: in the phosphate components (V_1 -958; V_2 -469; V_4 -556 cm^{-1}), in carbonate (V_2 -871 cm^{-1}), in the amide I + H_2O (1,646.41 cm^{-1}), amide II+ CO_3 (1,540.21 cm^{-1}), and amide III (1,237.70 cm^{-1}). All these parameters were significant when compared to the controls (Fig. 4).

The characterization of mineral components showed an increase in crystallinity after exposure to IHg

The characterization of mineral components by X-ray diffraction (XRD) showed a slight increase in the hydroxyapatite crystallinity in the alveolar bone after exposure to IHg. The comparison was made between the X-ray diffraction pattern of the alveolar bone of

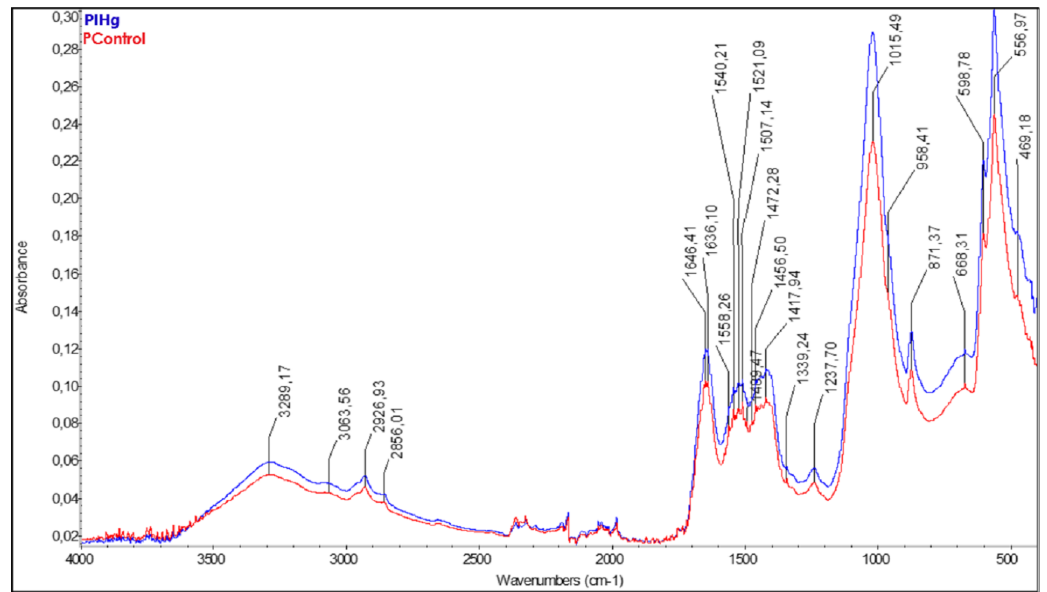


Figure 4 The characterization of organic and inorganic components presented changes in these parameters between groups (FT-IR). Effects of IHg exposure (0.375 mg/kg/day HgCl_2) during 45 days on FT-IR infrared spectroscopic profile analysis of alveolar bone of adult rats (90-days-old, $n = 10$ animals/group). The qualitative results were expressed by absorbance as a function of wavelength (cm^{-1}) in the comparison between FT-IR spectra of the control group (red line) with the exposed group (blue line). [Full-size !\[\]\(fd7fe780e8fd8eece60268c87d0c3e04_img.jpg\) DOI: 10.7717/peerj.12573/fig-4](https://doi.org/10.7717/peerj.12573/fig-4)

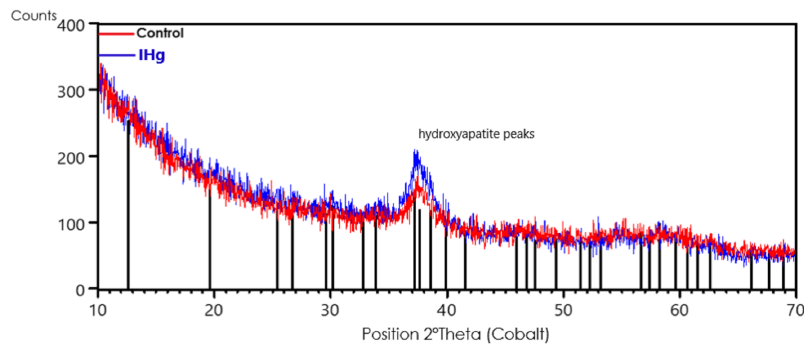


Figure 5 Effects of exposure to IHg (0.375 mg/kg/day HgCl_2) for 45 days on X-ray diffraction (XRD) analysis of hydroxyapatite in alveolar bone from adult rats (90 days of age, $n = \text{ten}$ animals/group). The characterization of mineral components showed an increase in crystallinity after exposure to IHg. Qualitative chemical results show the comparison between the XRD peak positions of the control group (red line) with the exposed group (blue line). The vertical black lines are the peak positions of the hydroxyapatite standard (ICDD-PDF 34-0011). [Full-size !\[\]\(86257f54800c9844bc7e863bea396fba_img.jpg\) DOI: 10.7717/peerj.12573/fig-5](https://doi.org/10.7717/peerj.12573/fig-5)

the control group (red line) with the IHg group (blue line). The vertical black lines are the peak positions of the hydroxyapatite standard (ICDD-PDF 34-0011).

The presence of hydroxyapatite with low intensity and wide peak at 37.2° in the control group and a slightly more intense and symmetrical peak in the exposed group shows, qualitatively, an increase in the crystallinity of the rats exposed to IHg, as shown in Fig. 5.

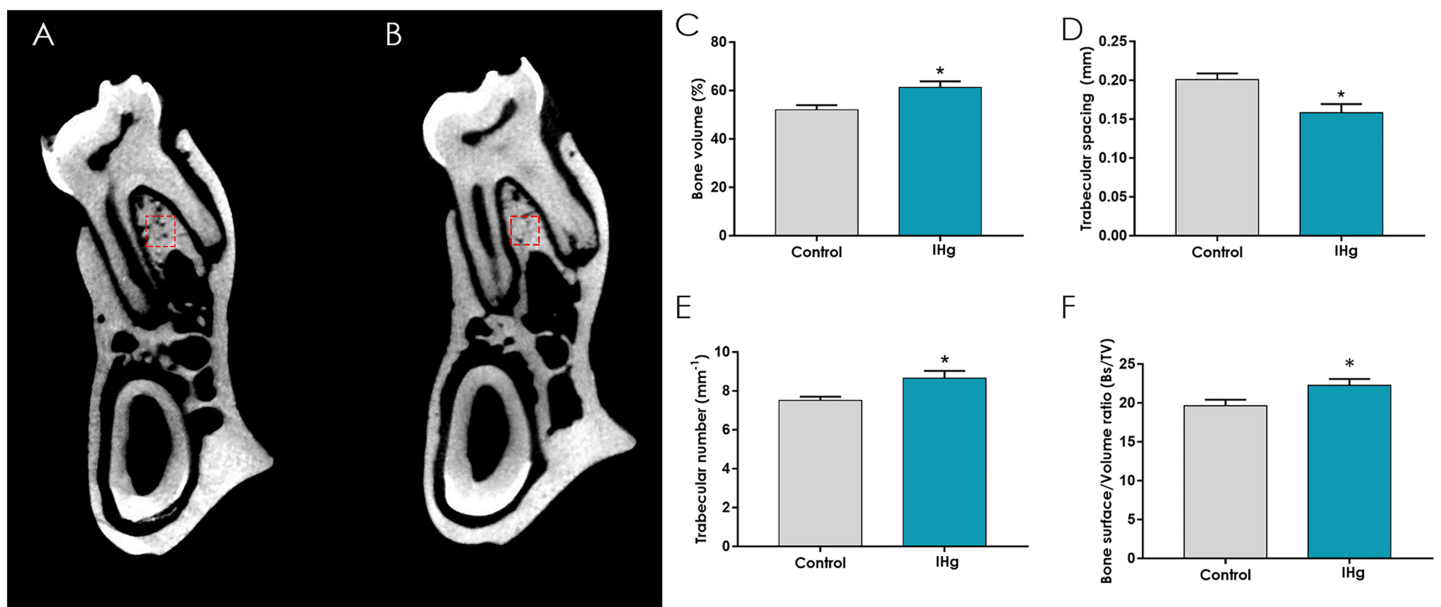


Figure 6 Effects of IHg exposure (0.375 mg/kg/day HgCl₂) during 45 days on the quality of the alveolar bone of adult rats (90-days-old). (A and B) The region of interest (ROI) was represented by the interradicular region on the furcation area. Image A represents the control group and B the exposed group. The micro-CT parameters used: (C) bone volume (BV/TV; %); (D) trabecular spacing (Tb.Sp; mm); (E) trabecular number (Tb.N; mm⁻¹); and (F) bone surface density (Bs/TV). Results are expressed as mean ± standard error mean. Student's *t*-test, * $p < 0.05$.

Full-size DOI: 10.7717/peerj.12573/fig-6

The exposure to IHg generated microstructural reactions in the alveolar bone

The micro-CT analysis revealed that long-term exposure to IHg could cause a change in the microstructure of the alveolar bone. Hence, the IHg was able to stimulate an increase in the trabecular number when compared to the control group (IHg: $0.86 \pm 0.37 \text{ mm}^{-1}$; Control: $0.75 \pm 0.19 \text{ mm}^{-1}$, respectively, $p = 0.04$, Fig. 6E), as well as a decrease in the space between the bone trabeculae in the exposed group (IHg: $0.15 \pm 0.01 \text{ mm}^{-1}$; Control: $0.20 \pm 0.007 \text{ mm}^{-1}$, respectively, $p = 0.01$, Fig. 6D).

Moreover, the alveolar bone showed a tissue response to the toxicant, increasing bone volume/bone surface (Bv/Tv) (IHg: 61.35 ± 2.49 ; Control: 52.04 ± 1.95 ; $p = 0.01$, Fig. 6C) and one of the density parameters bone, the fraction of the bone surface/volume ratio (Bs/Tv) (IHg: 22.28 ± 0.8 ; Control: 19.65 ± 0.7 ; $p = 0.04$, Fig. 6F) in the exposed group, as illustrated in the analyzed areas represented by A and B in Fig. 6.

Exposure to IHg for 45 days did not promote alveolar bone loss on the stereomicroscopy analysis

The stereomicroscopy revealed that the animals exposed to IHg did not show a significant difference in the exposed root area when compared to the control group (0.68 ± 0.01 ; 0.63 ± 0.01 ; $p > 0.05$) (Fig. 7).

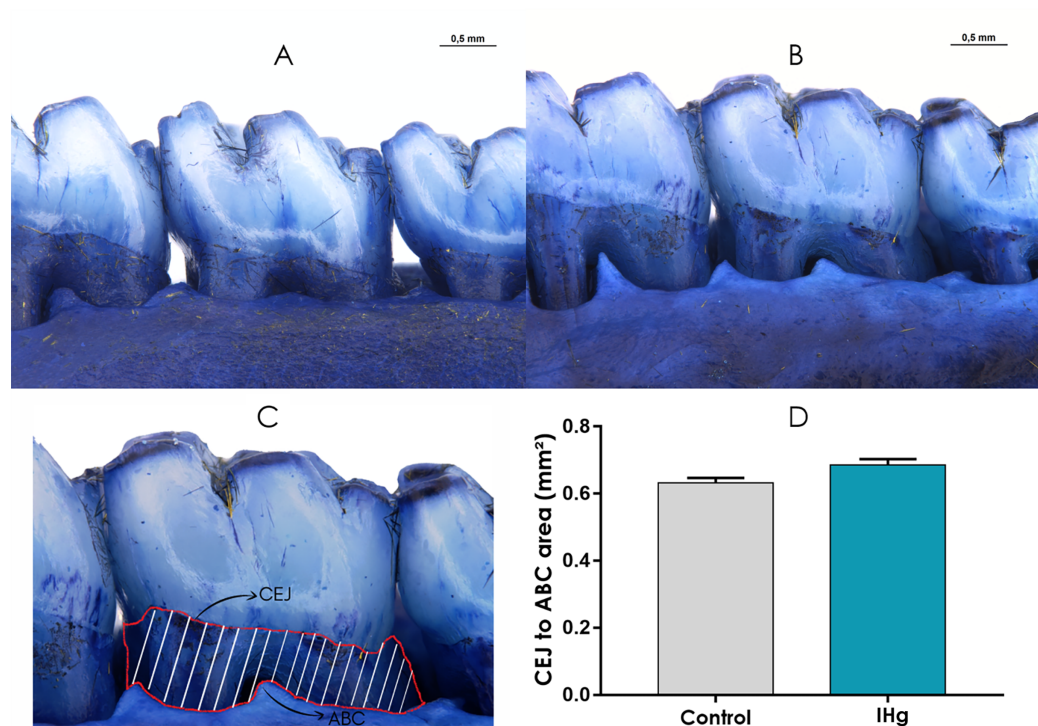


Figure 7 Photomicrographs of hemimandibles of the (A) control group, (B) exposed group, and (C) representative image of the exposed root area (traced in red). The graphic (D) represents the difference between the groups regarding the area between cemento enamel junction (CEJ) to alveolar bone crest (ABC) (mm²). Results are expressed as mean \pm standard error mean. Student's *t*-test, **p* < 0.05. Scale Bar: 0.5 mm. [Full-size !\[\]\(43e4e85f3e07c993849f98a1fa87e486_img.jpg\) DOI: 10.7717/peerj.12573/fig-7](https://doi.org/10.7717/peerj.12573/fig-7)

DISCUSSION

This study revealed that IHg exposure altered both organic and inorganic components of the alveolar bone and increased bone mineral crystallinity. Moreover, IHg triggered a microstructural change in the alveolar bone, modulated both bone integrity and volume, and consequently decreased trabecular space. These findings suggest that the Hg levels found in the blood of the exposed animals are related to the modulation of bone microstructure; however, the reaction against Hg did not result in significant changes in the alveolar bone dimension that provides tooth support.

Several studies from our research group have shown that this IHg exposure model caused changes in blood, central nervous system, and salivary glands (Aragão *et al.*, 2017; Aragão *et al.*, 2018; Teixeira *et al.*, 2018; Teixeira *et al.*, 2019; Corrêa *et al.*, 2020; Dos Santos Chemelo *et al.*, 2020). This study evidenced that the oral administration of IHg can trigger changes at biochemical and molecular levels (Lohren *et al.*, 2015; Aragão *et al.*, 2018; Corrêa *et al.*, 2020). Although Hg levels were not directly measured in the alveolar bone and considering the increased Hg concentrations in other tissues observed by previous studies, it can be suggested that Hg levels observed in the blood are associated with alveolar bone modulations.

It is worth mentioning that unlikely long bones, the alveolar bone has characteristics of compact bones such as fewer microporosities and a lower proportion of bone marrow (Monje *et al.*, 2015; Zhou *et al.*, 2018). Moreover, this tissue supports teeth that are subjected to continuous bone remodeling processes due to eruptions, occlusal forces, losses, periodontal diseases, and orthodontic movements (Tompkins, 2016). Therefore, the effects reported in long bones may differ from those observed in the alveolar bone.

Organic Hg species are predominantly reported in the literature since are widely found in contaminated fish and seafood (Rice *et al.*, 2014). When in contact with the clouds, the Hg vapor is partially converted into IHg. Once methylated, Hg can easily cross cell membranes and is promptly absorbed into the food chain (biomagnification and bioaccumulation) (Crespo-Lopez *et al.*, 2021; O'Connor *et al.*, 2019). Therefore, the combination of Hg dose and the high alveolar bone turnover rate can explain the modulation of crystallinity—distribution pattern of hydroxyapatites evaluated by the characteristic spectrum of these crystals—observed in this study. The diffractograms showed that IHg exposure modulated apatite crystals, which may have increased the structural components of alveolar bone as shown by micro-CT.

The modulation of carbonate, phosphate, and amides observed through ATR-FTIR indicates that IHg exposure can modulate mineralized tissues such as alveolar bone. Some organic (amides) and inorganic (carbonate and phosphate) components are increased as a response to tissue damage and evidence a repair process (Hassumi *et al.*, 2018). However, the increase of carbonate concentration observed in this study may be related to physical-chemical and morphological changes in mineralized tissues such as solubility increase, atomic positions variation, crystal morphology alteration, and bone mineral crystallinity decrease (Yerramshetty & Akkus, 2008; Morris & Mandair, 2011).

The literature shows that low concentrations of some metals such as zinc, copper, and nickel can play a role in bone modulation (Rodríguez & Mandalunis, 2018). Due to its morphological characteristics, the alveolar bone submitted to aggression can synthesize matrix components and increase mineralization (Zhou *et al.*, 2018); therefore, constant bone remodeling occurs through balanced levels of RANK/RANKL/OPG and alkaline phosphatase enzymes (Cao *et al.*, 2003; Tompkins, 2016; Hassumi *et al.*, 2018; Page-McCaw, Ewald & Werb, 2007). The micro-CT analysis revealed that long-term IHg exposure may increase both bone volume and density, and consequently decrease the trabecular space. This study's findings suggest that IHg was distributed throughout the body and affected the bone matrix; however, no adverse effects were observed due to protection mechanisms of the alveolar bone.

Since no significant difference in the pattern of alveolar bone loss was observed between groups, it seems that IHg can not induce horizontal and vertical loss without changing alveolar bone morphology. Thickness, height, and trabecular number are parameters that indicate the balance of the alveolar bone that support teeth (Shrout *et al.*, 2003; Ferrare *et al.*, 2013; Porto *et al.*, 2020); however, the alterations observed in micro-CT and mineral composition did not compromise bone dimensions.

The stereomicroscope analysis revealed that changes in the microstructure and mineral composition of the alveolar bone did not include vertical bone dimensions. Considering

that the alveolar bone vertical dimension is a relevant clinical parameter of bone health, the IHg exposure can be unnoticed for a certain period; therefore further studies with populations vulnerable to Hg exposure are encouraged.

CONCLUSIONS

IHg exposure did not cause vertical bone loss (from the cemento-enamel junction up to the alveolar bone crest), albeit modulation of physical-chemical components and microtomography parameters was observed. Despite the lack of dimension changes, the alveolar bone characterized by a high remodeling rate reacted to the toxicity of a low IHg dose.

ADDITIONAL INFORMATION AND DECLARATIONS

Funding

This study was supported by the Pró-Reitoria de Pesquisa (PACI/PROPESP/UFPA/Brazil), Brazilian National Council for Scientific and Technological Development (CNPq), Coordenação de Aperfeiçoamento de Pessoal de Nível Superior - Brazil (CAPES) – Finance Cod 001. The APC was funded by Pró-Reitoria de Pesquisa e Pós-graduação from Universidade Federal do Pará (PROPESP-UFPA). The funders had no role in study design, data collection and analysis, decision to publish, or preparation of the manuscript.

Grant Disclosures

The following grant information was disclosed by the authors:

Pró-Reitoria de Pesquisa (PACI/PROPESP/UFPA/Brazil).

Brazilian National Council for Scientific and Technological Development (CNPq).

Coordenação de Aperfeiçoamento de Pessoal de Nível Superior - Brazil (CAPES): 001.

Universidade Federal do Pará (PROPESP-UFPA).

Competing Interests

The authors declare that they have no competing interests.

Author Contributions

- Paula Beatriz de Oliveira Nunes conceived and designed the experiments, performed the experiments, analyzed the data, prepared figures and/or tables, authored or reviewed drafts of the paper, and approved the final draft.
- Maria Karolina Martins Ferreira conceived and designed the experiments, performed the experiments, analyzed the data, prepared figures and/or tables, authored or reviewed drafts of the paper, and approved the final draft.
- Deborah Ribeiro Frazão conceived and designed the experiments, prepared figures and/or tables, authored or reviewed drafts of the paper, and approved the final draft.
- Leonardo Oliveira Bittencourt conceived and designed the experiments, prepared figures and/or tables, authored or reviewed drafts of the paper, and approved the final draft.

- Victória dos Santos Chemelo conceived and designed the experiments, prepared figures and/or tables, authored or reviewed drafts of the paper, and approved the final draft.
- Marcia Freitas da Silva conceived and designed the experiments, analyzed the data, authored or reviewed drafts of the paper, and approved the final draft.
- Armando Lopes Pereira Neto analyzed the data, authored or reviewed drafts of the paper, and approved the final draft.
- Alan Rodrigo Leal Albuquerque analyzed the data, prepared figures and/or tables, and approved the final draft.
- Simone Patricia Aranha Paz conceived and designed the experiments, authored or reviewed drafts of the paper, and approved the final draft.
- Rômulo Simões Angélica conceived and designed the experiments, prepared figures and/or tables, and approved the final draft.
- Sofia Pessanha analyzed the data, authored or reviewed drafts of the paper, and approved the final draft.
- Rafael Rodrigues Lima conceived and designed the experiments, prepared figures and/or tables, authored or reviewed drafts of the paper, and approved the final draft.

Animal Ethics

The following information was supplied relating to ethical approvals (*i.e.*, approving body and any reference numbers):

Ethics Committee on Experimental Animals of the Federal University of Pará (UFPA) approved the study (9228050418).

Data Availability

The following information was supplied regarding data availability:

The raw measurements are available in the [Supplemental File](#).

Supplemental Information

Supplemental information for this article can be found online at <http://dx.doi.org/10.7717/peerj.12573#supplemental-information>.

REFERENCES

- Ahmad S, Mahmood R. 2019.** Mercury chloride toxicity in human erythrocytes: enhanced generation of ROS and RNS, hemoglobin oxidation, impaired antioxidant power, and inhibition of plasma membrane redox system. *Environmental Science and Pollution Research* **26**:5645–5657 DOI [10.1007/s11356-018-04062-5](https://doi.org/10.1007/s11356-018-04062-5).
- Aragão WAB, da Costa NMM, Fagundes NCF, Silva MCF, Alves-Junior SM, Pinheiro JJV, Amado LL, Crespo-López ME, Maia CSF, Lima RR. 2017.** Chronic exposure to inorganic mercury induces biochemical and morphological changes in the salivary glands of rats. *Metallomics* **9**(9):1271–1278 DOI [10.1039/C7MT00123A](https://doi.org/10.1039/C7MT00123A).
- Aragão WAB, Teixeira FB, Fagundes NCF, Fernandes RM, Fernandes LMP, da Silva MCF, Amado LL, Sagica FES, Oliveira EHC, Crespo-Lopez ME, Maia CSF, Lima RR. 2018.** Hippocampal dysfunction provoked by mercury chloride exposure: evaluation of cognitive impairment, oxidative stress, tissue injury and nature of cell death. *Oxidative Medicine and Cellular Longevity* **10**(7):1–11 DOI [10.1155/2018/7878050](https://doi.org/10.1155/2018/7878050).

- Ballatori N. 2002.** Transport of toxic metals by molecular mimicry. *Environ Health Perspect* **110**(Suppl. 5):689–694 DOI [10.1289/ehp.02110s5689](https://doi.org/10.1289/ehp.02110s5689).
- Bernhoft RA. 2012.** Mercury toxicity and treatment: a review of the literature. *Journal of Environmental and Public Health* **2012**:460508 DOI [10.1155/2012/460508](https://doi.org/10.1155/2012/460508).
- Bridges CC, Zalups RK. 2004.** Homocysteine, system b0,+ and the renal epithelial transport and toxicity of inorganic mercury. *American Journal of Pathology* **165**(4):1385–1394 DOI [10.1016/S0002-9440\(10\)63396-2](https://doi.org/10.1016/S0002-9440(10)63396-2).
- Bridges CC, Zalups RK. 2005.** Molecular and ionic mimicry and the transport of toxic metals. *Toxicology and Applied Pharmacology* **204**(3):274–308 DOI [10.1016/j.taap.2004.09.007](https://doi.org/10.1016/j.taap.2004.09.007).
- Bridges CC, Zalups RK. 2010.** Transport of inorganic mercury and methylmercury in target tissues and organs. *Journal of Toxicology and Environmental Health, Part B* **13**(5):385–410 DOI [10.1080/10937401003673750](https://doi.org/10.1080/10937401003673750).
- Cao J, Venton L, Sakata T, Halloran BP. 2003.** Expression of RANKL and OPG correlates with age-related bone loss in male C57BL/6 mice. *Journal of Bone and Mineral Research* **18**(2):270–277 DOI [10.1359/jbmr.2003.18.2.270](https://doi.org/10.1359/jbmr.2003.18.2.270).
- Corrêa MG, Bittencourt LO, Nascimento PC, Ferreira RO, Aragão WAB, Silva MCF, Gomes-Leal W, Fernandes MS, Dionizio A, Buzalaf MR, Crespo-Lopez ME, Lima RR. 2020.** Spinal cord neurodegeneration after inorganic mercury long-term exposure in adult rats: ultrastructural, proteomic and biochemical damages associated with reduced neuronal density. *Ecotoxicology and Environmental Safety* **191**(6):110159 DOI [10.1016/j.ecoenv.2019.110159](https://doi.org/10.1016/j.ecoenv.2019.110159).
- Crespo-Lopez ME, Augusto-Oliveira M, Lopes-Araújo A, Santos-Sacramento L, Yuki Takeda P, Macchi BM, do Nascimento JLM, Maia CSF, Lima RR, Arrifano GP. 2021.** Mercury: what can we learn from the Amazon? *Environment International* **146**(36):106223 DOI [10.1016/j.envint.2020.106223](https://doi.org/10.1016/j.envint.2020.106223).
- Dos Santos Chemelo V, Bittencourt LO, Aragão WAB, Dos Santos SM, Souza-Rodrigues RD, Ribeiro C, Monteiro MC, Lima RR. 2020.** Long-term exposure to inorganic mercury leads to oxidative stress in peripheral blood of adult rats. *Biological Trace Element Research* **199**(8):2992–3000 DOI [10.1007/s12011-020-02411-5](https://doi.org/10.1007/s12011-020-02411-5).
- de Oliveira Lopes G, Aragão WAB, Bittencourt LO, Puty B, Lopes AP, Dos Santos SM, Monteiro MC, de Oliveira EHC, da Silva MCF, Lima RR. 2021.** Imaging microstructural damage and alveolar bone loss in rats systemically exposed to methylmercury: first experimental evidence. *Biological Trace Element Research* **199**(10):3707–3717 DOI [10.1007/s12011-020-02492-2](https://doi.org/10.1007/s12011-020-02492-2).
- Ferrare N, Leite AF, Caracas HC, de Azevedo RB, de Melo NS, de Souza Figueiredo PT. 2013.** Cone-beam computed tomography and microtomography for alveolar bone measurements. *Surgical and Radiologic Anatomy* **35**(6):495–502 DOI [10.1007/s00276-013-1080-x](https://doi.org/10.1007/s00276-013-1080-x).
- Frazão DR, Maia CDSF, Chemelo VDS, Monteiro D, Ferreira RO, Bittencourt LO, Balbinot GS, Collares FM, Rösing CK, Martins MD, Lima RR. 2020.** Ethanol binge drinking exposure affects alveolar bone quality and aggravates bone loss in experimentally-induced periodontitis. *PLOS ONE* **15**(7):e0236161 DOI [10.1371/journal.pone.0236161](https://doi.org/10.1371/journal.pone.0236161).
- Hassumi JS, Mulinari-Santos G, Fabris RGM, Jacob A, Gonçalves AC, Rossi AR, Faverani FLP, Okamoto R. 2018.** Alveolar bone healing in rats: micro-CT, immunohistochemical and molecular analysis. *Journal of Applied Oral Science* **26**:e20170326 DOI [10.1590/1678-7757-2017-0326](https://doi.org/10.1590/1678-7757-2017-0326).
- Jin GB, Inoue S, Urano T, Cho S, Ouchi Y, Cyong JC. 2002.** Induction of anti-metallothionein antibody and mercury treatment decreases bone mineral density in mice. *Toxicology and Applied Pharmacology* **185**(2):98–110 DOI [10.1006/taap.2002.9531](https://doi.org/10.1006/taap.2002.9531).

- Lohren H, Blagojevic L, Fitkau R, Ebert F, Schildknecht S, Leist M, Schwerdtle T. 2015. Toxicity of organic and inorganic mercury species in differentiated human neurons and human astrocytes. *Journal of Trace Elements in Medicine and Biology* 32(3):200–208 DOI 10.1016/j.jtemb.2015.06.008.
- Lopes C, Limirio P, Novais V, Dechichi P. 2018. Fourier transform infrared spectroscopy (FTIR) application chemical characterization of enamel, dentin and bone. *Applied Spectroscopy Reviews* 53(9):1–23 DOI 10.1080/05704928.2018.1431923.
- Lopes Castro MM, Nascimento PC, Souza-Monteiro D, Santos SM, Arouck MB, Garcia VB, Araújo RF Jr, de Araujo AA, Balbinot GS, Collares FM, Rosing CK, Monteiro MC, Ferraz Maia CS, Lima RR. 2020. Blood oxidative stress modulates alveolar bone loss in chronically stressed rats. *International Journal of Molecular Sciences* 21(10):3728 DOI 10.3390/ijms21103728.
- Mavropoulos A, Rizzoli R, Ammann P. 2007. Different responsiveness of alveolar and tibial bone to bone loss stimuli. *Journal of Bone and Mineral Research* 22(3):403–410 DOI 10.1359/jbmr.061208.
- Monje A, Chan HL, Galindo-Moreno P, Elnayef B, Suarez-Lopez del Amo F, Wang F, Wang HL. 2015. Alveolar bone architecture: a systematic review and meta-analysis. *Journal of Periodontology* 86(11):1231–1248 DOI 10.1902/jop.2015.150263.
- Morris MD, Mandair GS. 2011. Raman assessment of bone quality. *Clinical Orthopaedics & Related Research* 469(8):2160–2169 DOI 10.1007/s11999-010-1692-y.
- O'Connor D, Hou D, Ok YS, Mulder J, Duan L, Wu Q, Wang S, Tack FMG, Rinklebe J. 2019. Mercury speciation, transformation, and transportation in soils, atmospheric flux, and implications for risk management: a critical review. *Environment International* 126(9):747–761 DOI 10.1016/j.envint.2019.03.019.
- Page-McCaw A, Ewald AJ, Werb Z. 2007. Matrix metalloproteinases and the regulation of tissue remodelling. *Nature Reviews Molecular Cell Biology* 8(3):221–233 DOI 10.1038/nrm2125.
- Park JD, Zheng W. 2012. Human exposure and health effects of inorganic and elemental mercury. *Journal of Preventive Medicine & Public Health* 45(6):344–352 DOI 10.3961/jpmph.2012.45.6.344.
- Percie du Sert N, Ahluwalia A, Alam S, Avey MT, Baker M, Browne WJ, Clark A, Cuthill IC, Dirnagl U, Emerson M, Garner P, Holgate ST, Howells DW, Hurst V, Karp NA, Lazic SE, Lidster K, MacCallum CJ, Macleod M, Pearl EJ, Petersen OH, Rawle F, Reynolds P, Rooney K, Sena ES, Silberberg SD, Steckler T, Würbel H. 2020. Reporting animal research: explanation and elaboration for the ARRIVE guidelines 2.0. *PLOS Biology* 18(7):e3000411 DOI 10.1371/journal.pbio.3000411.
- Porto OCL, Silva BSF, Silva JA, Estrela CRA, Alencar AHG, Bueno MDR, Estrela C. 2020. CBCT assessment of bone thickness in maxillary and mandibular teeth: an anatomic study. *Journal of Applied Oral Science* 28(5):e20190148 DOI 10.1590/1678-7757-2019-0148.
- Rice KM, Walker EM Jr, Wu M, Gillette C, Blough ER. 2014. Environmental mercury and its toxic effects. *Journal of Preventive Medicine & Public Health* 47(2):74–83 DOI 10.3961/jpmph.2014.47.2.74.
- Rodríguez J, Mandalunis PM. 2018. A review of metal exposure and its effects on bone health. *Journal of Toxicology* 2018:4854152 DOI 10.1155/2018/4854152.
- Rodríguez Martín-Doimeadios RC, Berzas Nevado JJ, Guzmán Bernardo FJ, Jiménez Moreno M, Arrifano GP, Herculano AM, do Nascimento JL, Crespo-López ME. 2014. Comparative study of mercury speciation in commercial fishes of the Brazilian Amazon.

- Environmental Science and Pollution Research* **21(12)**:7466–7479
DOI [10.1007/s11356-014-2680-7](https://doi.org/10.1007/s11356-014-2680-7).
- Risher JF, De Rosa CT. 2007.** Inorganic: the other mercury. *Journal of Environmental Health* **70(4)**:9–16 discussion 40.
- Shrout MK, Jett S, Mailhot JM, Potter BJ, Borke JL, Hildebolt CF. 2003.** Digital image analysis of cadaver mandibular trabecular bone patterns. *Journal of Periodontology* **74(9)**:1342–1347
DOI [10.1902/jop.2003.74.9.1342](https://doi.org/10.1902/jop.2003.74.9.1342).
- Sakamoto M, Nakamura M, Murata K. 2018.** Mercury as a global pollutant and mercury exposure assessment and health effects. *Nihon Eiseigaku Zasshi* **73(3)**:258–264 DOI [10.1265/jjh.73.258](https://doi.org/10.1265/jjh.73.258).
- Siciliano SD, O'Driscoll NJ, Tordon R, Hill J, Beauchamp S, Lean DR. 2005.** Abiotic production of methylmercury by solar radiation. *Environmental Science & Technology* **39(4)**:1071–1077
DOI [10.1021/es048707z](https://doi.org/10.1021/es048707z).
- Tanaka M, Ejiri S, Toyooka E, Kohno S, Ozawa H. 2002.** Effects of ovariectomy on trabecular structures of rat alveolar bone. *Journal of Periodontal Research* **37(2)**:161–165
DOI [10.1034/j.1600-0765.2002.01601.x](https://doi.org/10.1034/j.1600-0765.2002.01601.x).
- Teixeira FB, de Oliveira ACA, Leão LKR, Fagundes NCF, Fernandes RM, Fernandes LMP, da Silva MCF, Amado LL, Sagica FES, de Oliveira EHC, Crespo-Lopez ME, Maia CSF, Lima RR. 2018.** Exposure to inorganic mercury causes oxidative stress, cell death, and functional deficits in the motor cortex. *Frontiers in Molecular Neuroscience* **11**:125
DOI [10.3389/fnmol.2018.00125](https://doi.org/10.3389/fnmol.2018.00125).
- Teixeira FB, Fernandes RM, Farias-Junior PM, Costa NM, Fernandes LM, Santana LN, Silva-Junior AF, Silva MC, Maia CS, Lima RR. 2014.** Evaluation of the effects of chronic intoxication with inorganic mercury on memory and motor control in rats. *International Journal of Environmental Research and Public Health* **11(9)**:9171–9185
DOI [10.3390/ijerph110909171](https://doi.org/10.3390/ijerph110909171).
- Teixeira FB, Leão LKR, Bittencourt LO, Aragão WAB, Nascimento PC, Luz DA, Braga DV, Silva M, Oliveira KRM, Herculano AM, Maia CSF, Lima RR. 2019.** Neurochemical dysfunction in motor cortex and hippocampus impairs the behavioral performance of rats chronically exposed to inorganic mercury. *Journal of Trace Elements in Medicine and Biology* **52(12)**:143–150 DOI [10.1016/j.jtemb.2018.12.008](https://doi.org/10.1016/j.jtemb.2018.12.008).
- Tompkins KA. 2016.** The osteoimmunology of alveolar bone loss. *Connective Tissue Research* **57(2)**:69–90 DOI [10.3109/03008207.2016.1140152](https://doi.org/10.3109/03008207.2016.1140152).
- UNEP. 2013.** *Global mercury assessment 2013: sources, emission, releases and environmental transport*. Geneva: UNEP Chemicals Branch.
- WHO. 2017.** *Mercury and health*. Geneva: WHO.
- Yerramshetty JS, Akkus O. 2008.** The associations between mineral crystallinity and the mechanical properties of human cortical bone. *Bone* **42(3)**:476–482
DOI [10.1016/j.bone.2007.12.001](https://doi.org/10.1016/j.bone.2007.12.001).
- Zhou S, Yang Y, Ha N, Zhang P, Ma X, Gong X, Hong Y, Yang X, Yang S, Dai Q, Jiang L. 2018.** The specific morphological features of alveolar bone. *Journal of Craniofacial Surgery* **29(5)**:1216–1219 DOI [10.1097/SCS.0000000000004395](https://doi.org/10.1097/SCS.0000000000004395).